NASA/TM—2015-218738

Analysis of Turbine Blade Relative Cooling Flow Factor Used in the Subroutine Coolit Based on Film Cooling Correlations

Steven J. Schneider
Glenn Research Center, Cleveland, Ohio

June 2015

NASA STI Program . . . in Profile

Since its founding, NASA has been dedicated to the advancement of aeronautics and space science. The NASA Scientific and Technical Information (STI) Program plays a key part in helping NASA maintain this important role.

The NASA STI Program operates under the auspices of the Agency Chief Information Officer. It collects, organizes, provides for archiving, and disseminates NASA's STI. The NASA STI Program provides access to the NASA Technical Report Server—Registered (NTRS Reg) and NASA Technical Report Server—Public (NTRS) thus providing one of the largest collections of aeronautical and space science STI in the world. Results are published in both non-NASA channels and by NASA in the NASA STI Report Series, which includes the following report types:

- TECHNICAL PUBLICATION. Reports of completed research or a major significant phase of research that present the results of NASA programs and include extensive data or theoretical analysis. Includes compilations of significant scientific and technical data and information deemed to be of continuing reference value. NASA counter-part of peer-reviewed formal professional papers, but has less stringent limitations on manuscript length and extent of graphic presentations.

- TECHNICAL MEMORANDUM. Scientific and technical findings that are preliminary or of specialized interest, e.g., "quick-release" reports, working papers, and bibliographies that contain minimal annotation. Does not contain extensive analysis.

- CONTRACTOR REPORT. Scientific and technical findings by NASA-sponsored contractors and grantees.

- CONFERENCE PUBLICATION. Collected papers from scientific and technical conferences, symposia, seminars, or other meetings sponsored or co-sponsored by NASA.

- SPECIAL PUBLICATION. Scientific, technical, or historical information from NASA programs, projects, and missions, often concerned with subjects having substantial public interest.

- TECHNICAL TRANSLATION. English-language translations of foreign scientific and technical material pertinent to NASA's mission.

For more information about the NASA STI program, see the following:

- Access the NASA STI program home page at http://www.sti.nasa.gov

- E-mail your question to help@sti.nasa.gov

- Fax your question to the NASA STI Information Desk at 757-864-6500

- Telephone the NASA STI Information Desk at 757-864-9658

- Write to:
  NASA STI Program
  Mail Stop 148
  NASA Langley Research Center
  Hampton, VA 23681-2199

NASA/TM—2015-218738

Analysis of Turbine Blade Relative Cooling Flow Factor Used in the Subroutine Coolit Based on Film Cooling Correlations

Steven J. Schneider
Glenn Research Center, Cleveland, Ohio

National Aeronautics and
Space Administration

Glenn Research Center
Cleveland, Ohio 44135

June 2015

Level of Review: This material has been technically reviewed by technical management.

Available from

NASA STI Program
Mail Stop 148
NASA Langley Research Center
Hampton, VA 23681-2199

National Technical Information Service
5285 Port Royal Road
Springfield, VA 22161
703-605-6000

This report is available in electronic form at http://www.sti.nasa.gov/ and http://ntrs.nasa.gov/

Analysis of Turbine Blade Relative Cooling Flow Factor Used in the Subroutine Coolit Based on Film Cooling Correlations

Steven J. Schneider
National Aeronautics and Space Administration
Glenn Research Center
Cleveland, Ohio 44135

Abstract

Heat transfer correlations of data on flat plates are used to explore the parameters in the Coolit program used for calculating the quantity of cooling air for controlling turbine blade temperature. Correlations for both convection and film cooling are explored for their relevance to predicting blade temperature as a function of a total cooling flow which is split between external film and internal convection flows. Similar trends to those in Coolit are predicted as a function of the percent of the total cooling flow that is in the film. The exceptions are that no film or 100 percent convection is predicted to not be able to control blade temperature, while leaving less than 25 percent of the cooling flow in the convection path results in nearing a limit on convection cooling as predicted by a thermal effectiveness parameter not presently used in Coolit.

Nomenclature

	Description	*Units*	*Example*
A	flow area	m^2	varies
a	sonic velocity	m/s	varies
B	distance between blades	m	0.02
C_1	convection from combustion gas	W/m^2	varies
C_2	convection to cooling air	W/m^2	varies
D_c	cooling passage width	m	varies
D_h	hydraulic diameter of cooling passage	m	varies
FAC	relative cooling flow factor in Coolit[1]		varies
h	convective heat transfer coefficient	W/m^2 K	varies
H	height of blades	m	0.05
k_c	thermal conductivity of cooling air	W/m K	0.0553
k_g	thermal conductivity of combustion gas	W/m K	0.164
L	length of blade in flow direction	m	0.05
m	momentum ratio ($\rho_c U_c/\rho_g U_g$)		varies
M_c	cooling flow Mach number		0.3
M_g	combustion flow Mach number		0.6
$\dot{m}_c$	mass flow of cooling air	kg/s	varies
$\dot{m}_g$	mass flow of combustion gas	kg/s	varies
$\dot{m}_s$	mass flow in film cooling layer	kg/s	varies
$\dot{m}_{tot}$	total mass flow	kg/s	varies

P	pressure	kPa	varies
P_{tc}	cooling flow inlet total pressure	kPa	3040
P_{tg}	combustion gas inlet total pressure	kPa	3040
Pr	Prandtl Number		varies
Re_{cDh}	Reynolds No. based hydraulic diameter		varies
Re_{gx}	Reynolds No. based on axial distance		varies
Re_s	Reynolds No. based on slot height		varies
s	film cooling slot height	m	varies
T_{tc}	cooling flow inlet total temperature	K	880
T_{tg}	combustion gas total temperature	K	2280
T_{aw}	adiabatic wall temperature of blade	K	varies
T_w	wall temperature	K	varies
U	uniform velocity	m/s	varies
x	axial distance from cooling slot	m	varies
α	fraction of cooling flow in convection		varies
γ_c	specific heat ratio of cooling gas		1.4
γ_g	specific heat ratio of combustion gas		1.25
η_x	film-cooling effectiveness		varies
η_{conv}	thermal effectiveness of convection (Eq. (3))		varies
μ_c	viscosity of cooling air	kg/m/s	3.89e-5
μ_g	viscosity of combustion gas	kg/m/s	7.41e-5
ρ	density of gas	kg/m^3	varies
ϕ	cooling effectiveness of wall (Eq. (2))		varies

Subscripts:

c	pertaining to cooling flow
g	pertaining to combustion flow
i	pertaining to coolant inlet
o	pertaining to coolant outlet
s	pertaining to static flow conditions
t	pertaining to total flow conditions
x	pertaining to axial position along blade

Analytic Procedure

A methodology based on a combination of film cooling and internal convection cooling is used to check the relative cooling flow factors in the Coolit (Ref. 1) subroutine which is used for estimating turbine cooling flow requirements. The relative cooling flow factor (FAC) is chosen during a Coolit analysis to estimate dimensionless cooling as a function of desired blade temperature using the following equations.

$$\frac{\dot{m}_c}{\dot{m}_g} = 0.022\,\mathrm{FAC}\left(\frac{\phi}{1-\phi}\right)^{1.25} \tag{1}$$

The cooling effectiveness ϕ is defined by the following equation, which gives a relationship between combustion gas temperature, cooling gas temperature, and desired wall temperature.

$$\phi = \frac{T_{tg} - T_w}{T_{tg} - T_{tc}} \tag{2}$$

Equation (1) is a curve fit to data (Ref. 2) for a full coverage film cooled vane where FAC = 1 is assumed in Coolit.

There is also a thermal effectiveness parameter (Ref. 3) η_{conv} that is monitored in this analysis and may be useful to monitor in Coolit as well. It is a measure of how close the wall temperature is to the coolant temperature at the outlet of the internal convection path. It is calculated as a cooling performance indicator in this analysis. It is defined as follows

$$n_{\text{conv}} = \frac{T_{tco} - T_{tci}}{T_{wo} - T_{tci}} \tag{3}$$

Convection Cooling Only Case

The internal convection only case is analyzed using Figure 1.

Convective heat transfer per unit area (C_2) inside the blade is modeled by empirical data in the form of heat transfer coefficients (h) in fully turbulent pipe flow (Re_{cDh}>2300), which is easy to achieve in blade passages, but should always be checked. Correlations in the form of Nusselt Numbers are used to model specific data sets.

$$Nu_{D_h} = \frac{h_c D_h}{k_c} = 0.023\,\text{Re}_{cD_h}^{0.8}\,\text{Pr}_c^{0.4} \tag{4}$$

where

$$\text{Re}_{cDh} = \frac{\dot{m}_c D_h}{A_c \mu_c} \tag{5}$$

and

$$A_c = \frac{\dot{m}_c a_c}{\rho_{sc} M_c} \tag{6}$$

and

$$D_h = \frac{2A_c}{H + D_c} \tag{7}$$

The convective heat transfer per unit area inside the blade is then

$$C_2(x) = h_c\left[T_w(x) - T_{tc}(x)\right] = 0.023\frac{k_c}{D_h}\text{Re}_{cD_h}^{0.8}\,\text{Pr}_c^{0.4}\left[T_w(x) - T_{tc}(x)\right] \tag{8}$$

Convective heat transfer per unit area (C_1) outside the blade is modeled by correlations of turbulent flow over a flat plate at constant temperature. The local Nusselt Number correlation is as follows for turbulent flow with Reynolds Numbers $5\times10^5<\mathrm{Re}_{gx}<10^7$,which can be difficult to achieve near the leading edge of the blade, but is used here with that caveat.

$$Nu_{gx} = \frac{h_g x}{k_g} = 0.0292\,\mathrm{Re}_{gx}^{0.8}\,\mathrm{Pr}_g^{1/3} \tag{9}$$

where

$$\mathrm{Re}_{gx} = \frac{\rho_{sg} U_g x}{\mu_g} \tag{10}$$

and

$$U_g = \frac{M_g}{a_g} \tag{11}$$

The convective heat transfer per unit area on the outside of the blade is then a function of axial position as follows.

$$C_1(x) = h_g(x)\left[T_{tg} - T_w(x)\right] = 0.0292\frac{k_g}{x}\mathrm{Re}_{gx}^{0.8}\,\mathrm{Pr}_g^{1/3}\left[T_{tg} - T_w(x)\right] \tag{12}$$

Neglecting axial conduction $C_1(x) = C_2(x)$ and for simplicity assuming zero wall thickness leads to the following equation for wall temperature as a function of axial position.

$$T_w(x) = \frac{0.0292\frac{k_g}{x}\mathrm{Re}_{gx}^{0.8}\,\mathrm{Pr}_g^{1/3}\,T_{tg} + 0.023\frac{k_c}{D_h}\mathrm{Re}_{cD_h}^{0.8}\,\mathrm{Pr}_c^{0.4}\,T_{tc}(x)}{0.0292\frac{k_g}{x}\mathrm{Re}_{gx}^{0.8}\,\mathrm{Pr}_g^{1/3} + 0.023\frac{k_c}{D_h}\mathrm{Re}_{cD_h}^{0.8}\,\mathrm{Pr}_c^{0.4}} \tag{13}$$

The blade length (L) is then divided into N increments of $\Delta x = L/N$ and integrated numerically with the flow of heat across the wall increasing the coolant flow temperature (T_{tc}) as a function of axial position (x), but with the combustion gas temperature (T_{tg}) remaining unchanged. Heat flows in from both sides of the blade into the i_{th} increment of Δx according to the following equation.

$$2C_{1i(x)} = \frac{\dot{m}_c C_{pc}}{H\Delta x}\left(T_{tc_{i+1}} - T_{tc_i}\right) \tag{14}$$

Substituting for $C_1(x)$ and solving for T_{tci+1} the increase in cooling temperature flow is obtained.

$$T_{tc_{i+1}} = T_{tc_i} + \frac{2H\Delta x}{\dot{m}_c C_{pc}} 0.0292\frac{k_g}{x}\mathrm{Re}_{gx}^{0.8}\,\mathrm{Pr}_g^{1/3}\left[T_{tg} - T_w(x)\right] \tag{15}$$

These equations are then numerically integrated for heat flux $C_1(x)$, coolant flow temperature $T_{tc}(x)$, and wall temperature $T_w(x)$.

Film and Convection Cooling Case

The external film cooling using slot cooling and internal convection cooling case is analyzed using the Figure 2 schematic shown below. Only the flow downstream of the slot is modeled. The leading edge is not modeled. Since a row of holes is typically used on a turbine blade, it would have to be converted to an equivalent slot width for use with the slot correlations. In this case only the fraction α of the total coolant flow $\dot{m}_c$ flows through the blade and the remainder fraction 1-α is used for film cooling.

Convective heat transfer per unit area (C_2) inside the blade is again modeled by empirical data in the form of heat transfer coefficients (h) in fully turbulent pipe flow using Equations (4) and (8).

where the Reynolds Number is now

$$\mathrm{Re}_{cDh} = \frac{a\dot{m}_c D_h}{A_c \mu_c} \tag{16}$$

and the convection coolant flow area is

$$A_c = \frac{a\dot{m}_c a_c}{\rho_{sc} M_c} \tag{17}$$

Convective heat transfer per unit area (C_1) outside the blade is modeled by correlations of turbulent film cooling, which alters heat transfer by both a velocity and temperature change near the wall. Correlations (Ref. 4) have been developed to account for both effects.

Dealing with the velocity first, a momentum ratio of the coolant flow to hot gas flow is defined as follows

$$m = \frac{\rho_{sc} U_c}{\rho_{sg} U_g} \tag{18}$$

Values of this parameter separate flow regimes identified as boundary layer and wall jet regimes in film cooling analyses.

Boundary Layer Flow Regime

The boundary layer regime is estimated to occur between $0.5<m<1.3$ with the following correlation

$$Nu_{gx} = \frac{h_g x}{k_g} = 0.069\left(\mathrm{Re}_s \frac{x}{s}\right)^{0.7} \tag{19}$$

where the Reynolds Number based on slot width s is defined as follows

$$\mathrm{Re}_s = \frac{\rho_{sc} U_c s}{\mu_c} \tag{20}$$

The convective heat transfer per unit area on the outside of the blade as a function of axial position is then as follows.

$$C_1(x) = h_g(x)\left[T_{aw}(x) - T_w(x)\right] = 0.069\frac{k_g}{x}\left(\mathrm{Re}_s\frac{x}{s}\right)^{0.7}\left[T_{aw}(x) - T_w(x)\right] \tag{21}$$

Neglecting axial conduction $C_1(x) = C_2(x)$ and for simplicity assuming zero wall thickness leads to the following equation for wall temperature as a function of axial position.

$$T_w(x) = \frac{0.069\frac{k_g}{x}\left(\mathrm{Re}_s\frac{x}{s}\right)^{0.7}T_{aw}(x) + 0.023\frac{k_c}{D_h}\mathrm{Re}_{D_h}^{0.8}\,\mathrm{Pr}_c^{0.4}\,T_{tc}(x)}{0.069\frac{k_g}{x}\left(\mathrm{Re}_s\frac{x}{s}\right)^{0.7} + 0.023\frac{k_c}{D_h}\mathrm{Re}_{D_h}^{0.8}\,\mathrm{Pr}_c^{0.4}} \tag{22}$$

The effect of temperature change due to film cooling near the wall is taken into account by defining the adiabatic wall temperature T_{aw} used in Equations (21) and (22) in lieu of using the total gas temperature T_{tg}. The adiabatic wall temperature T_{aw} is obtained from correlations of the film-cooling effectiveness parameter η_x as follows.

$$\eta_x = \frac{T_{tg} - T_{aw(x)}}{T_{tg} - T_{tc}} \tag{23}$$

Different correlations (Ref. 4) exist for the near slot region and the region far downstream of the slot. The near slot region is defined by $0<x/s<150$ with the following correlation

$$\eta_x = 0.6\left(\frac{x}{ms}\right)^{-0.3}\left(\mathrm{Re}_s\frac{m\mu_c}{\mu_g}\right)^{0.15} \tag{24}$$

Data for this correlation was also limited to $0.5<m<1.3$, $0.8<\rho_{sc}/\rho_{sg}<2.5$, and $0.0019<s<0.0064$ m. The far downstream correlation defined by $x/s>150$ is given by the following correlation.

$$\eta_x = 3.68\left(\frac{x}{ms}\right)^{-0.8}\left(\mathrm{Re}_s\frac{\mu_c}{\mu_g}\right)^{0.2} \tag{25}$$

Wall Jet Regime

The wall jet regime is estimated to occur at $m>1.3$ with the following correlation

$$\mathrm{Nu}_{gx} = \frac{h_g x}{k_g} = 0.10\,\mathrm{Re}_s^{0.8}\left(\frac{x}{s}\right)^{0.44} \tag{26}$$

The convective heat transfer per unit area on the outside of the blade as a function of axial position for this case is then as follows.

$$C_1(x) = h_g(x)\left[T_{aw}(x) - T_w(x)\right] = 0.10\frac{k_g}{x}\mathrm{Re}_s^{0.8}\left(\frac{x}{s}\right)^{0.44}\left[T_{aw}(x) - T_w(x)\right] \tag{27}$$

Again, neglecting axial conduction $C_1(x) = C_2(x)$ and for simplicity assuming zero wall thickness leads to the following equation for wall temperature as a function of axial position.

$$T_w(x) = \frac{0.10\frac{k_g}{x}\mathrm{Re}_s^{0.8}\left(\frac{x}{s}\right)^{0.44}T_{aw}(x) + 0.023\frac{k_c}{D_h}\mathrm{Re}_{D_h}^{0.8}\,\mathrm{Pr}_c^{0.4}\,T_{tc}(x)}{0.10\frac{k_g}{x}\mathrm{Re}_s^{0.8}\left(\frac{x}{s}\right)^{0.44} + 0.023\frac{k_c}{D_h}\mathrm{Re}_{D_h}^{0.8}\,\mathrm{Pr}_c^{0.4}} \tag{28}$$

Again, the effect of temperature change due to film cooling near the wall is taken into account by defining the adiabatic wall temperature T_{aw} used in Equations (27) and (28) in lieu of using the total gas temperature T_{tg}. The adiabatic wall temperature T_{aw} is obtained from correlations of the film-cooling effectiveness parameter η_x defined by Equation (23). Different correlations (Ref. 4) exist for different flow regimes as follows

For the regime defined by $0<x/s<150$ and $1.3<m<4$ and $x/ms<8$

$$n_x = 1.0 \tag{29}$$

For the flow regime defined by $0<x/s<150$ and $1.3<m<4$ and $8<x/ms<11$

$$\eta_x = \left(0.6 + 0.05\frac{x}{ms}\right)^{-1} \tag{30}$$

For the regime defined by $0<x/s<150$ and $1.3<m<4$ and $x/ms>11$

$$\eta_x = 0.7\left(\frac{x}{s}\right)^{-0.3}\left(\mathrm{Re}_s\frac{\mu_c}{\mu_g}\right)^{0.15}(m)^{-0.2} \tag{31}$$

For the far downstream regime $x/s>150$ the correlation given by Equation (25) is used again.

The blade length (L) is again divided into N increments of $\Delta x = L/N$ and the equations are integrated numerically with the flow of heat across the wall increasing the coolant flow temperature (T_{tc}) as a function of axial position (x), and the adiabatic wall temperature T_{aw} also varying with (x). Heat flows in from both sides of the blade into the i_{th} increment of Δx according to Equation (14). In the boundary layer regime between $0.5<m<1.3$ substituting Equation (21) for $C_1(x)$ and solving for T_{tci+1} the increase in cooling temperature flow is obtained.

$$T_{tc_{i+1}} = T_{tc_i} = \frac{2H\Delta x}{\dot{m}_c C_{pc}}0.069\frac{k_c}{x}\left(\mathrm{Re}_s\frac{x}{s}\right)^{0.7}\left[T_{aw}(x) - T_w(x)\right] \tag{32}$$

The wall jet regime at m>1.3 substitutes Equation (27) for $C_1(x)$ and solving for T_{tci+1} the increase in cooling flow temperature is obtained.

$$T_{tc_{i+1}} = T_{tc_i} + \frac{2H\Delta x}{\dot{m}_c C_{pc}} 0.10 \frac{k_c}{x} \mathrm{Re}_s^{0.8} \left(\frac{x}{s}\right)^{0.44} \left[T_{aw}(x) - T_w(x)\right] \tag{33}$$

These equations are then numerically integrated for heat flux $C_1(x)$, coolant flow temperature $T_{tc}(x)$, adiabatic wall temperature $T_{aw}(x)$, and wall temperature $T_w(x)$.

Solution Procedure

These equations are integrated over 0<X<L for the example parameters given in the nomenclature section and the results are given in Figures 3 through 9. Both an excel spreadsheet and a Fortran program given in Appendix A with an example input file in Appendix B are provided. Note that the balance of heat flux can be changed by varying the flow Mach Numbers. For these calculations the hot combustion flow has a Mach Number M_g = 0.6, whereas the cold coolant flow has a Mach Number of M_c = 0.3. A summary of the results and a comparison of the Coolit assumptions is given in Table 1 with further discussion below.

Figure 3(a) shows cooling flow outlet temperature T_{tco} which decreases as cooling flow increases. It also shows the wall inlet and outlet temperatures, T_{wi} and T_{wo}, respectively, which remain above 1750 K. This calculation says that pipe flow type convection cooling by itself cannot reduce the wall temperature much below 1750 K when the combustion temperature is 2280 K. The use of fin type structures inside the blade can enhance the cooling, but that is not analyzed here. Figure 3(b) plots the parameters η_{conv}, ϕ, and FAC from Equations (3), (2), and (1), respectively. The desired value of ϕ for a 1400 K wall temperature with 2280 K combustion temperature and 880 K cooling flow temperature is ϕ = 0.626, which is never reached in this calculation. The current use of FAC = 2 in Coolit estimates that there is only a factor of 2 difference between the cooling flow required for a blade with convection cooling only vs. a blade with a full coverage film. Unless there are significant coolant enhancement features inside the blade, this could grossly underestimate cooling requirements with convection only. Figure 3(c) gives the wall temperature profiles as a function of axial position at dimensionless cooling flow rates of 0.1, 0.2, and 0.4. If the combustion gas temperature is reduced to 1680 K, then the 1400 K wall temperature is possible as shown in Figure 4 where ϕ = 0.349, $\dot{m}_c / \dot{m}_g$ = 0.033, FAC = 3.27, and η_{conv} = 0.322.

In order to compare the film cooling analysis of Equations (16) to (33) with the 100 percent convection cooling analysis of Equations (4) to (15), a film cooling analysis with 98 percent convection and 2 percent film cooling is given in Figure 5 at 2280 K combustion temperature for comparison with Figure 3. There are some slight differences, but the wall temperature remains above 1750 K in agreement with that of Figure 3. Also, when the combustion gas temperature is reduced to T_g = 1680 K in Figure 6, the film cooling prediction is $\dot{m}_c / \dot{m}_g$ = 0.023, FAC = 2.28, and η_{conv} = 0.445. These numbers are at least comparable to those of Figure 4, in spite of the fact that this is a gross extrapolation of the film coolant data in that the slot dimensions are three orders of magnitude smaller than those used in the data correlations.

The 75 percent convection 25 percent film cooling case at T_g = 2280 K is shown in Figure 7. The effect of the film cooling effectiveness parameter η_x is shown by adiabatic wall temperature at the inlet (x = 0) and outlet (x = L) of the cooling passage, T_{awi} and T_{awo}, respectively in Figure 7(a). This reduction in temperature from 2280 K significantly reduces the heat flux and resulting wall temperature. The 1400 K wall temperature T_{wo} is reached with $\dot{m}_c / \dot{m}_g$ = 0.059 as shown in Figure 7(a) and FAC = 1.40 as shown in Figure 7(b). They are listed in Table 1. This case is in good agreement with the Coolit prediction of $\dot{m}_c / \dot{m}_g$ = 0.054 calculated by Equation (1) for FAC = 1.3 given in Coolit. The thermal

effectiveness parameter η_{conv} calculated using Equation (3), however, is only 0.166 whereas in Reference 3, where it is defined, only data above 0.5 is referenced. This indicates that the cooling flow for this case may be used more effectively. The calculated wall temperature for different mass flow ratios $\dot{m}_c / \dot{m}_g$ is shown as a function of axial position along the blade in Figure 7(c). It shows that when one correlation is handed off to another as *x* increases the transition is not always smooth.

The 50 percent convection 50 percent film cooling case at 2280 K is shown in Figure 8. In this case the 1400 K wall temperature is reached with $\dot{m}_c / \dot{m}_g$ = 0.032 and FAC = 0.766 as shown in the Figures 8(a) and (b) and listed in Table 1. This compares with the Coolit prediction of $\dot{m}_c / \dot{m}_g$ = 0.050 for FAC = 1.2 used in Coolit. Since Coolit is anchored in full coverage film coolant data from Reference 2 where FAC = 1.0, this film coolant data where FAC<1.0, suggests that a thick high velocity film leads to lower coolant massflow requirements indicating that it is more effective in cooling the blade than the full coverage film injected through a perforated surface. The thermal effectiveness parameter η_{conv} = 0.408, calculated using Equation (3) is still low for this case when compared to those reported in Reference 3 (η_{conv}>0.5).

The 25 percent convection 75 percent film cooling case at 2280 K is shown in Figure 9. In this case the 1400 K wall temperature is reached with $\dot{m}_c / \dot{m}_g$ = 0.023 and FAC = 0.550 as shown in the Figures 9(a) and (b) and listed in Table 1. This compares with the Coolit prediction of $\dot{m}_c / \dot{m}_g$ = 0.046 for FAC = 1.1 used in Coolit. Again, since Coolit is anchored in full coverage film coolant data from Reference 2 where FAC = 1.0, this film coolant data where FAC<1.0, suggests that a thick high velocity film leads to lower coolant massflow requirements than the full coverage film injected through a perforated surface. The thermal effectiveness parameter η_{conv} = 0.803, calculated using Equation (3) is comparable to those reported in Reference 3 (η_{conv}>0.5) in this case.

Conclusions

The use of flat plate film and convection cooling correlations predicts the trends currently employed for cooling analysis in Coolit, but should be considered optimistic due to their ideal nature, since injecting the film through a row of holes rather than a slot would increase turbulent heat transfer as would the positive pressure gradients within the blades due to their thinning of the boundary layers. The baseline in Coolit (FAC = 1.0) is the data set obtained in a full coverage film cascade experiment. The use of flat plate film correlations, perhaps optimistically, predicts that a thick uniform film introduced through a row of holes can reduce heat transfer (FAC<1.0) below that of the full coverage film introduced through holes distributed evenly over the whole surface. A detailed cascade experiment would be needed to prove this, however. This analysis does show that care must be taken in the Coolit assumptions when assuming that a blade is cooled by convection only in that overheating is possible. Also, at the opposite extreme, assuming that the bulk of the cooling flow is diverted from convection within the blade to a film cooling layer on the blade could lead to overheating of the convection coolant. An additional parameter not presently monitored in Coolit is the thermal effectiveness parameter given by Equation (3). This parameter matches the heat flux into the blade with the rise in temperature of the convection cooling within the blade. It would be wise to monitor this parameter in a Coolit analysis to show that excess cooling is not being employed for a given cooling configuration.

TABLE 1.—FOLLOWING AN EXAMPLE IN REFERENCE 4, RESULTS FOR 3040 KPA, 2280 K COMBUSTION FLOW WITH 880 K COOLING FLOW TO ACHIEVE 1400 K WALL TEMPERATURE, i.e., $\phi = 0.626$ WITH RESULTS USING COOLIT IN PARENTHESES

	100% convection cooled	75% convection 25% film	50% convection 50% film	25% convection 75% film
$\dot{m}_c / \dot{m}_g$	Not possible (0.084)	0.059 (0.054)	0.032 (0.050)	0.023 (0.046)
FAC	Not possible (2.0)	1.4 (1.3)	0.766 (1.2)	0.550 (1.1)
η_{conv}	Not possible	0.166	0.408	0.803

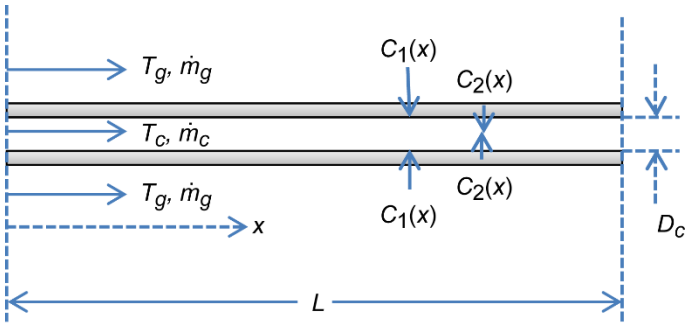

Figure 1.—Schematic showing convection-cooled passages.

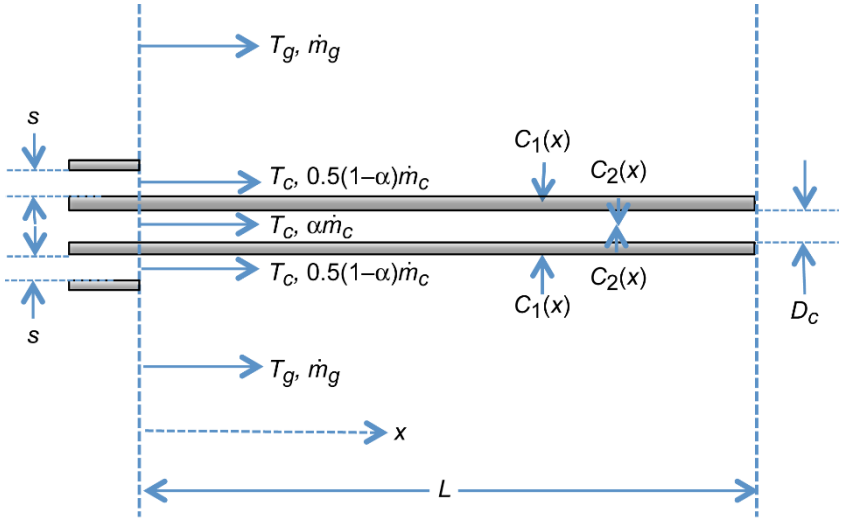

Figure 2.—Schematic showing external film cooling with a slot and internal convection cooling.

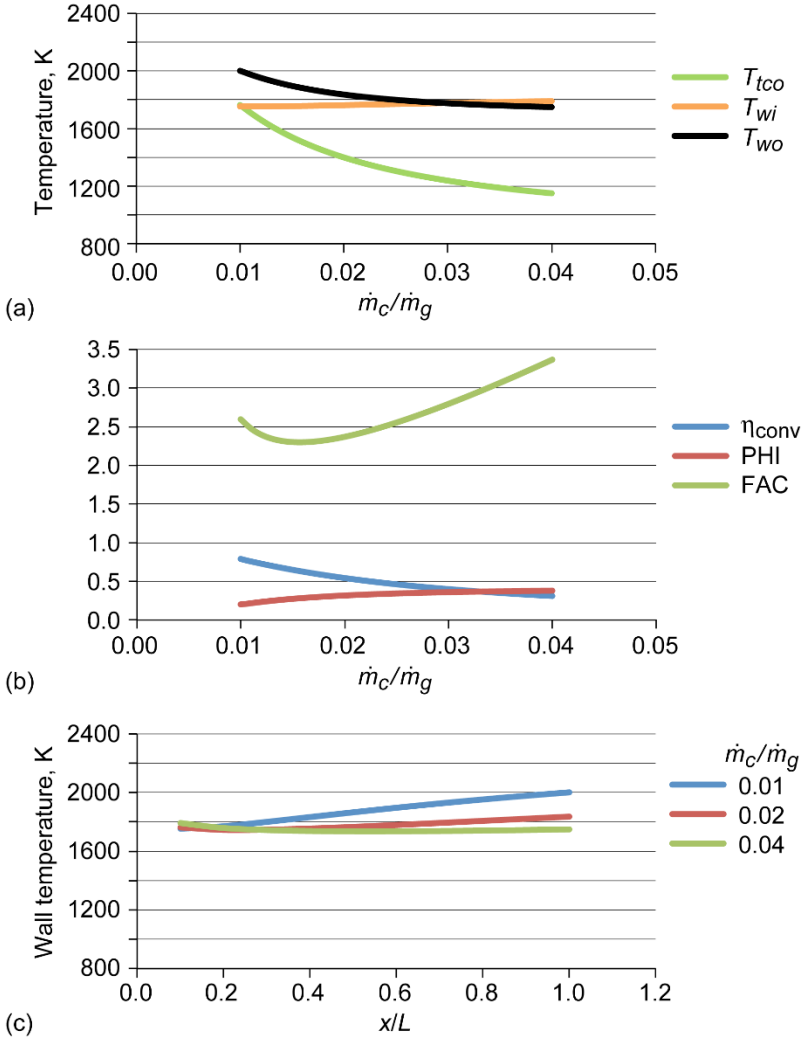

Figure 3.—Heat transfer with convection cooling (T_g = 2280 K) only. (a) Inlet and outlet wall and cooling flow outlet temperatures versus cooling flow. (b) Thermal effectiveness of convection, cooling effectiveness of wall, and relative cooling flow factor versus cooling flow. (c) Wall temperature as a function of axial position for several cooling flows.

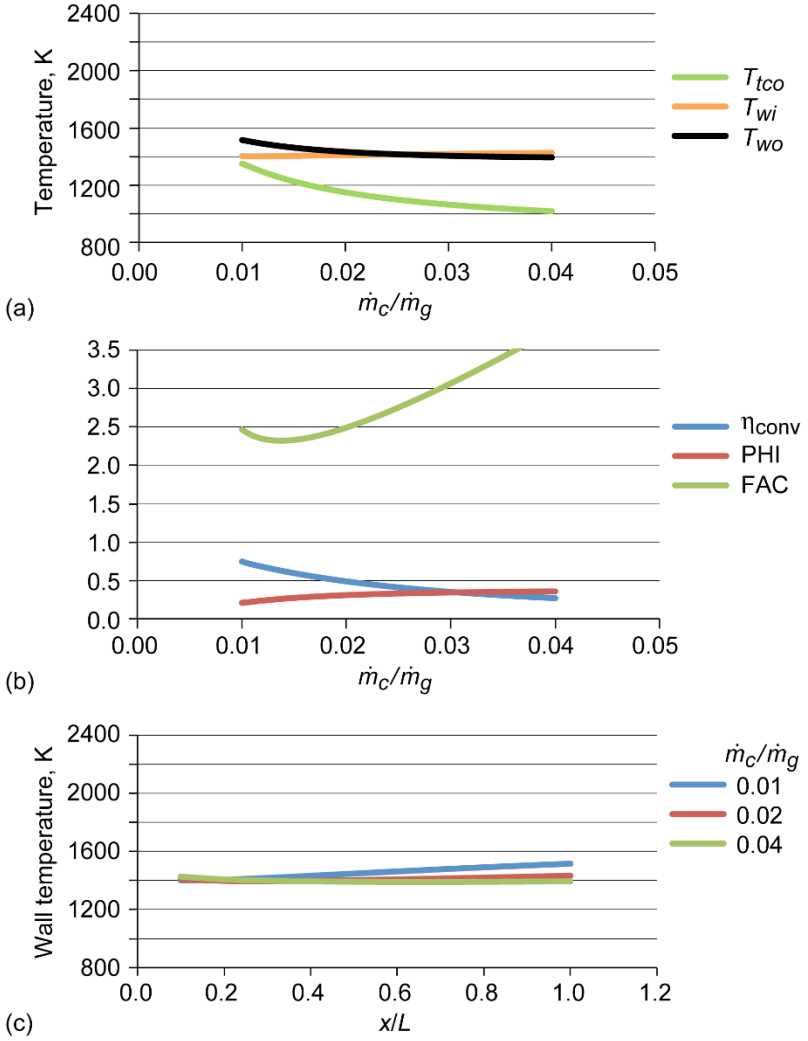

Figure 4.—Heat transfer with convection cooling (T_g = 1680 K) only. (a) Inlet and outlet wall and cooling flow outlet temperatures versus cooling flow. (b) Thermal effectiveness of convection, cooling effectiveness of wall, and relative cooling flow factor versus cooling flow. (c) Wall temperature as a function of axial position for several cooling flows.

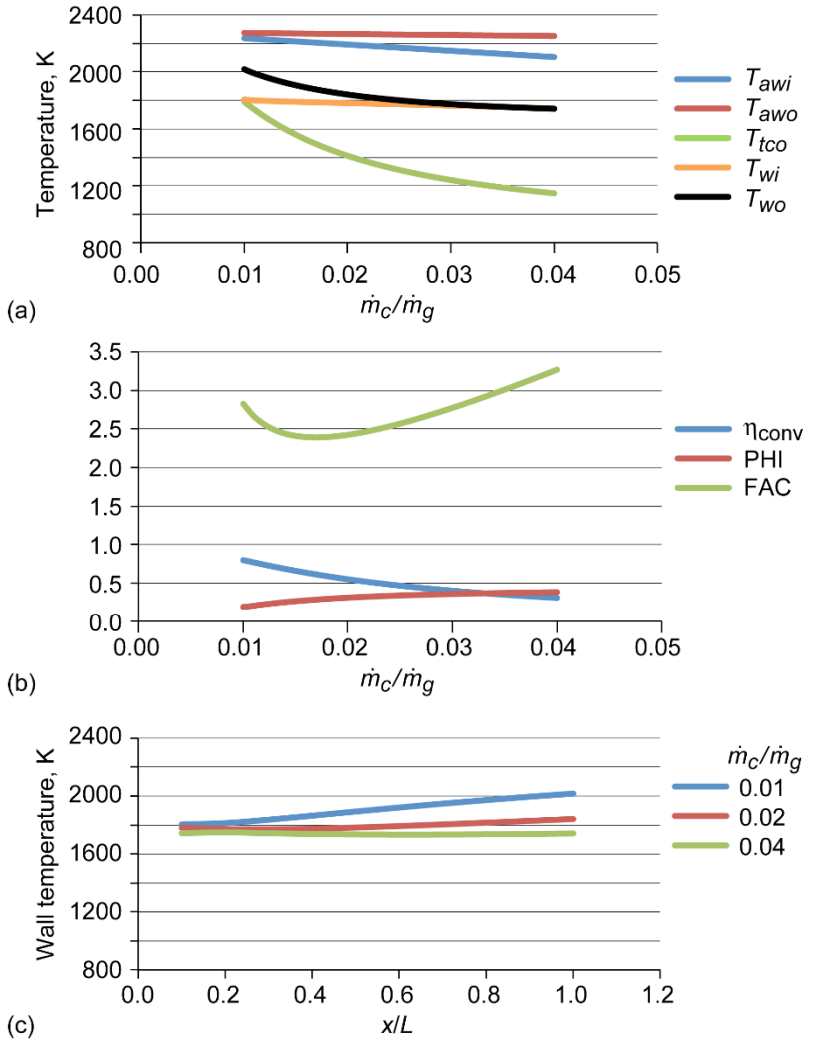

Figure 5.—Heat transfer with 98 percent convection and 2 percent film cooling used for model comparison with the convection (T_g = 2280 K) only model. (a) Inlet and outlet wall and cooling flow outlet temperatures versus cooling flow. (b) Thermal effectiveness of convection, cooling effectiveness of wall, and relative cooling flow factor versus cooling flow. (c) Wall temperature as a function of axial position for several cooling flows.

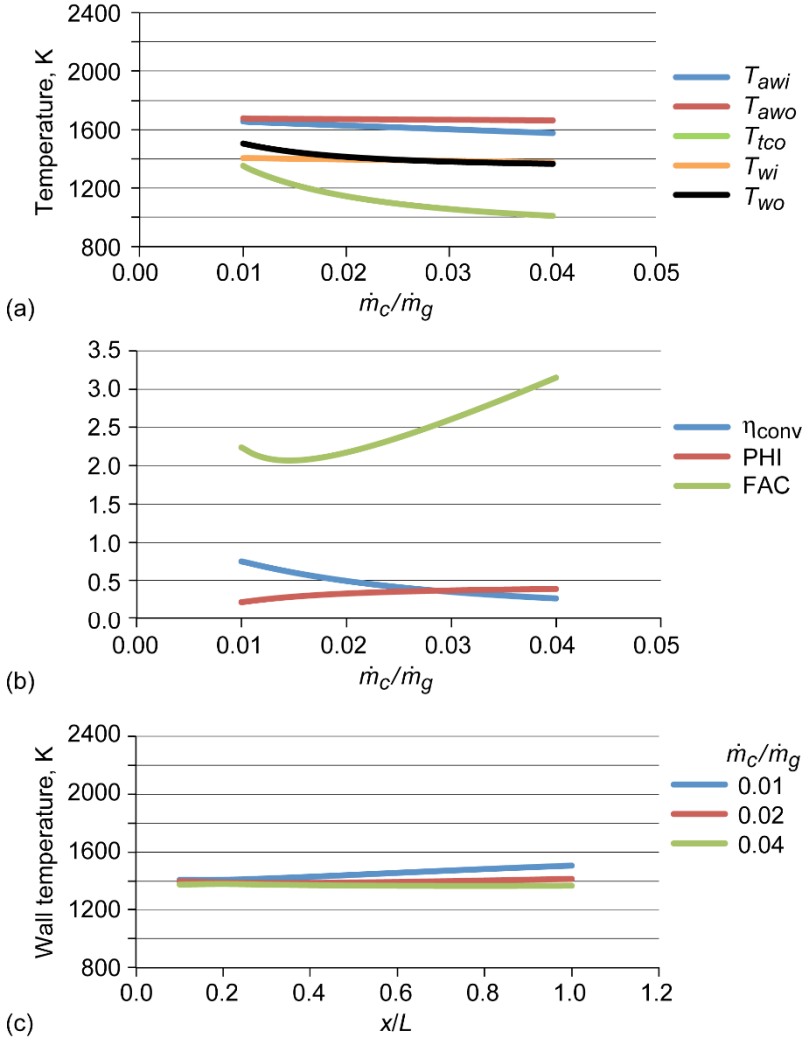

Figure 6.—Heat transfer with 98 percent convection and 2 percent film cooling used for model comparison with the convection (T_g = 1680 K) only model. (a) Inlet and outlet wall and cooling flow outlet temperatures versus cooling flow. (b) Thermal effectiveness of convection, cooling effectiveness of wall, and relative cooling flow factor versus cooling flow. (c) Wall temperature as a function of axial position for several cooling flows.

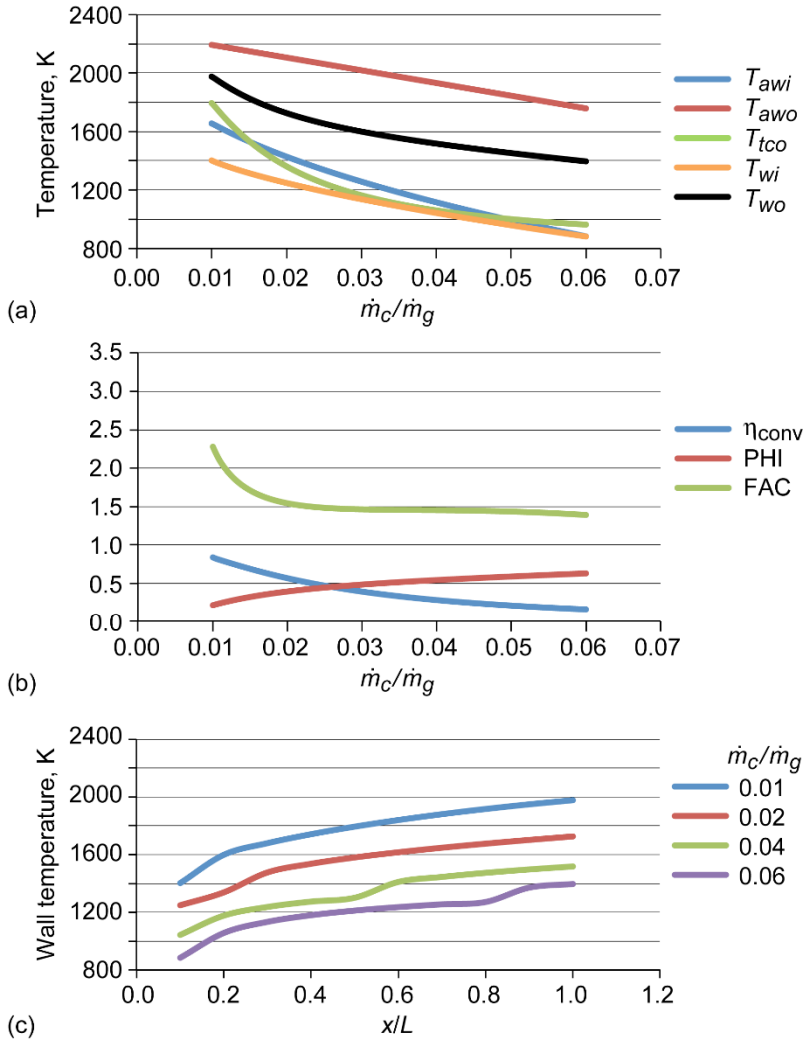

Figure 7.—Heat transfer with 75 percent convection and 25 percent film cooling (T_g = 2280 K). (a) Inlet and outlet wall and cooling flow outlet temperatures versus cooling flow. (b) Thermal effectiveness of convection, cooling effectiveness of wall, and relative cooling flow factor versus cooling flow. (c) Wall temperature as a function of axial position for several cooling flows.

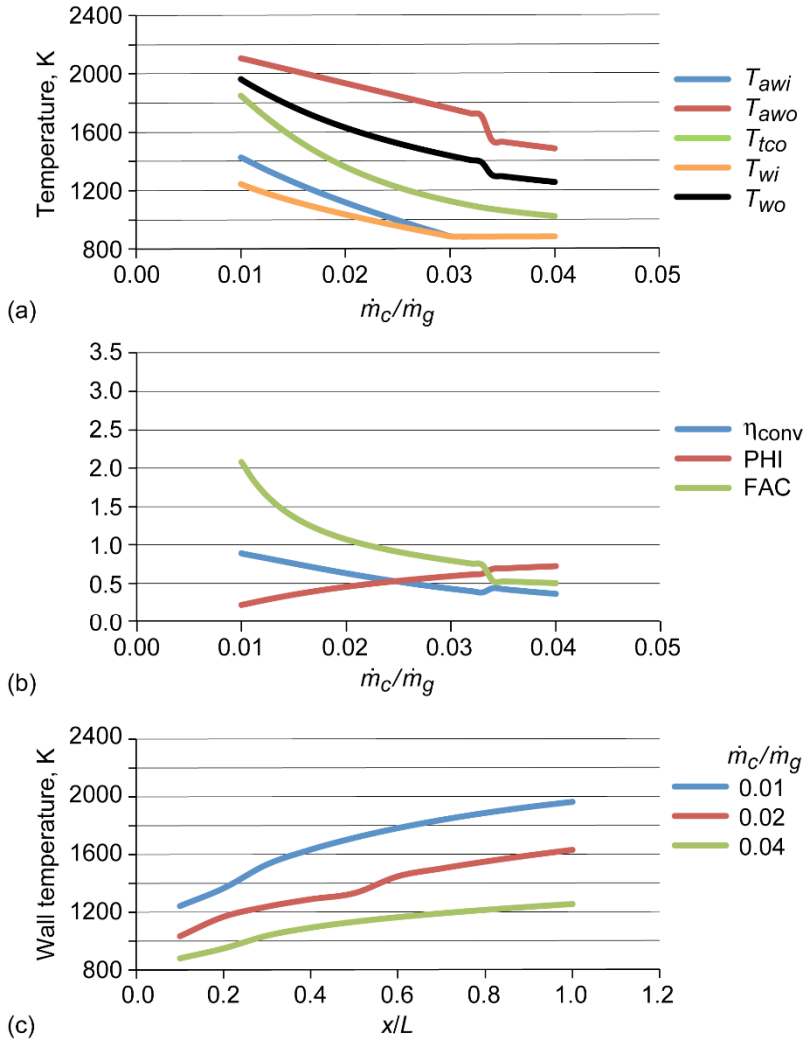

Figure 8.—Heat transfer with 50 percent convection and 50 percent film cooling (T_g = 2280 K). (a) Inlet and outlet wall and cooling flow outlet temperatures versus cooling flow. (b) Thermal effectiveness of convection, cooling effectiveness of wall, and relative cooling flow factor versus cooling flow. (c) Wall temperature as a function of axial position for several cooling flows.

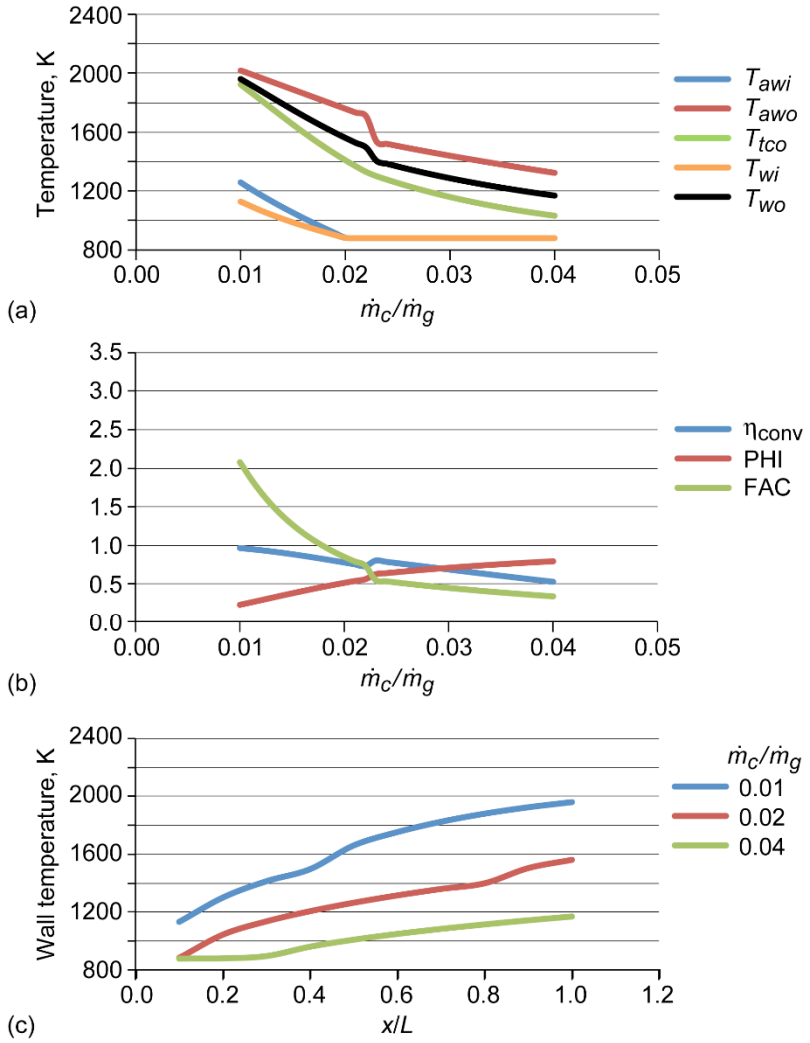

Figure 9.—Heat transfer with 25 percent convection and 75 percent film cooling (T_g = 2280 K). (a) Inlet and outlet wall and cooling flow outlet temperatures versus cooling flow. (b) Thermal effectiveness of convection, cooling effectiveness of wall, and relative cooling flow factor versus cooling flow. (c) Wall temperature as a function of axial position for several cooling flows.

Appendix A.—Fortran Source Code

```
      PROGRAM MAIN   !Turbine Blade Cooling Flow Calculation
      CHARACTER*80 INPUTFILE, OUTPUTFILE
!     Kase=1 is Convection Cooled Only, KASE=2 is Film Cooled and Convection Cooled
      REAL KC,MUC,MWC,KG,MUG,MWG,LEN,MOMR,MASSR,MACHG,MACHC,MG,MC,MTOT,MS
      REAL MASSRI,MASSRF
      DIMENSION TW(100)
      DOUBLE PRECISION ETAX,REGX,TWI,TAWX,TTC,C1,C2,A,B,TW
      NAMELIST/INPT1/KASE,PTG,TTG,KG,MWG,GAMG,MACHG,MUG
      NAMELIST/INPT2/PTC,TTC,KC,MWC,GAMC,MACHC,MUC
      NAMELIST/INPT3/RBAR,LEN,WID,HT,ALPHA,MASSRI,MASSRF,DMASSR,N,NPRINT
!     DATA PTC,TTC,KC,MUC/3040.,880.,0.0553,3.89E-5/
!     DATA MWC,GAMC,MACHC/28.95,1.4,0.6/
!     DATA PTG,TTG,KG/3040.,2280.,0.164/
!     DATA MUG,MWG,GAMG,MACHG/7.41E-5,27.76,1.25,0.6/
!     DATA RBAR,LEN,WID,HT/8314.,0.05,0.02,0.05/
!     DATA MASSR,N,NPRINT/0.108,1000,10/
!     DATA KASE,ALPHA/2,0.85/
      WRITE(*,*)
      WRITE(*,'(a)') ' HTBLD'
      WRITE(*,'(a,$)') '  Enter HTBLD input data file: '
      READ(*,'(a)') inputfile
      WRITE(*,'(a,$)') ' Enter HTBLD output data file: '
      READ(*,'(a)') outputfile
      open(5,file=inputfile,status='unknown',form='formatted')
      open(6,file=outputfile,status='unknown',form='formatted')
      READ(5,INPT1)
      READ(5,INPT2)
      READ(5,INPT3)
      NBET=N/NPRINT
      TSG=TTG/(1.+(GAMG-1.)/2.*MACHG*MACHG)
      TSC=TTC/(1.+(GAMC-1.)/2.*MACHC*MACHC)
      UG=MACHG*SQRT(GAMG*RBAR/MWG*TSG)
      UC=MACHC*SQRT(GAMC*RBAR/MWC*TSC)
      VELR=UC/UG
      RHOTG=PTG/RBAR*MWG/TTG*1000.
      RHOTC=PTC/RBAR*MWC/TTC*1000.
      CPC=GAMC*RBAR/MWC/(GAMC-1.)
      CPG=GAMG*RBAR/MWG/(GAMG-1.)
      RHOSG=RHOTG/(TTG/TSG)**(1./(GAMG-1.))
      RHOSC=RHOTC/(TTC/TSC)**(1./(GAMC-1.))
      DENSR=RHOSC/RHOSG
      PSG=PTG/(TTG/TSG)**(GAMG/(GAMG-1.))
      PSC=PTC/(TTC/TSC)**(GAMC/(GAMC-1.))
      AG=HT*WID
      MG=RHOSG*UG*AG
      IM=(MASSRF-MASSRI)/DMASSR+2
```

```
      MASSR=MASSRI
      TTCI=TTC
      DO 300 II=1,IM
      MC=MASSR*MG
      RHOSGUG=RHOSG*UG
      RHOSCUC=RHOSC*UC
      MOMR=RHOSCUC/RHOSGUG
      PRG=MUG*CPG/KG
      RHOSCUC=MOMR*RHOSGUG
      AC=MC/RHOSCUC
      IF(KASE.EQ.2)AC=ALPHA*MC/RHOSCUC
      DC=AC/HT
      MTOT=MC+MG
      PRC=MUC*CPC/KC
      DX=LEN/REAL(N)
      DH=2.0*AC/(HT+DC)
      RECDH=MC*DH/AC/MUC
      IF(KASE.EQ.2)RECDH=ALPHA*MC*DH/AC/MUC
      MS=MC*(1.-ALPHA)
      US=UC
      AS=MS/RHOSC/US
      S=AS/HT
      ALPHAMC=ALPHA*MC
      RES=RHOSC*US*S/MUC
      X=DX
      TTC=TTCI
      DO 200 J=1,NPRINT
      DO 100 I=1,NBET
      IF(KASE.EQ.1)GO TO 90
      XOS=X/S
      XOMS=X/MOMR/S
      IF(MOMR.GT.1.3)GO TO 91
      ETAX=0.6*(1./XOMS)**0.3*(RES*MOMR*MUC/MUG)**0.15
      IF(MOMR.LE.1.3)GO TO 92
   91 IF(XOS.LE.150.0.AND.XOMS.LE.8.0)ETAX=1.0
      IF(XOS.LE.150.0.AND.XOMS.GT.8.0)ETAX=1./(0.6+0.05*XOMS)
      IF(XOS.LE.150.0.AND.XOMS.GE.11.)ETAX=0.7*XOS**(-0.3)*(RES*MUC/MUG)**0.15*MOMR**(-0.2)
   92 IF(XOS.GT.150.)ETAX=3.68*(1./XOMS)**0.8*(RES*MUC/MUG)**0.2
      IF(ETAX.GT.1.)ETAX=1.
      TAWX=TTG-ETAX*(TTG-TTCI)
      IF(J.EQ.1.AND.I.EQ.NBET)TAWXI=TAWX
   90 REGX=RHOSG*UG*X/MUG
      IF(KASE.EQ.1)A=0.0292*KG/X*REGX**0.8*PRG**(1./3.)
      IF(KASE.EQ.2.AND.MOMR.LE.1.3)A=0.069*KG/X*(RES*X/S)**0.7
      IF(KASE.EQ.2.AND.MOMR.GT.1.3)A=0.1*RES**0.8*KG/X*XOS**0.44
      B=0.023*KC/DH*RECDH**0.8*PRC**0.4
      IF(KASE.EQ.1)TWI=(A*TTG+B*TTC)/(A+B)
      IF(KASE.EQ.2)TWI=(A*TAWX+B*TTC)/(A+B)
```

```
      IF(KASE.EQ.1)C1=A*(TTG-TWI)
      IF(KASE.EQ.2)C1=A*(TAWX-TWI)
      C2=B*(TWI-TTC)
      TTCOLD=TTC
      IF(KASE.EQ.1)TTC=TTC+2.0*C1*HT*DX/MC/CPC
      IF(KASE.EQ.2)TTC=TTC+2.0*C1*HT*DX/ALPHA/MC/CPC
      XOLD=X
  100 X=X+DX
  200 TW(J)=TWI
      TTCO=TTC
      ETACONV=(TTCO-TTCI)/(TWI-TTCI)
      PHI=(TTG-TWI)/(TTG-TTCI)
      FAC=MASSR/0.022/(PHI/(1.-PHI))**1.25
      WRITE(6,30)MASSR,ETACONV,PHI,FAC,TAWXI,TAWX,TTCO,(TW(IJ),IJ=1,NPRINT)
  300 MASSR=MASSR+DMASSR
   30 FORMAT(1X,4F8.4,13F8.1)
      close(5)
      close(6)
      STOP
      END
```

Appendix B.—Namelist Input for 75 Percent Convection Cooling Case

```
NAMELISTS
$INPT1
KASE=2
PTG=3040.
TTG=2280.
KG=0.164
MWG=27.76
GAMG=1.25
MACHG=0.6
MUG=7.41E-05
$END
$INPT2
PTC=3040.
TTC=880.
KC=0.0553
MWC=28.95
GAMC=1.4
MACHC=0.3
MUC=3.89E-05
$END
$INPT3
RBAR=8314.
LEN=0.05
WID=0.02
HT=0.05
ALPHA=0.75
MASSRI=0.01
MASSRF=0.06
DMASSR=0.001
N=1000
NPRINT=10
$END
```

References

1. Gauntner, J.W., Algorithm for Calculating Turbine Cooling Flow and the Resulting Decrease in Turbine Efficiency, NASA-TM-81453, February 1980.
2. Livingood, J.N.B., Ellerbrock, H.H., and Kaufman, A., 1971 NASA Turbine Cooling Research Status Report, Figure 23 of NASA-TMX-2384, September 1971.
3. Esgar, J.B., Colladay, R.S., and Kaufman, A., An Analysis of the Capabilities and Limitations of Turbine Air Cooling Methods, NASA-TND-5992, September 1970.
4. Lefebvre, A.H., Gas Turbine Combustion, Chapter 8. Heat Transfer, Taylor and Francis Publishers, 1983.